

Investigation of the drawing mechanism of UHMWPE fibers

Jen-Taut Yeh · Shui-Chuan Lin · Cheng-Wei Tu ·
Kuo-Huang Hsie · Feng-Chih Chang

Received: 16 January 2008 / Accepted: 7 May 2008 / Published online: 3 June 2008
© Springer Science+Business Media, LLC 2008

Abstract The influence of draw ratios (DR) of gel-spun ultrahigh molecular weight polyethylene (UHMWPE) fibers on resultant morphologies, tensile, degrees of orientation, and crystal phase transition properties were investigated using wide-angle X-ray diffraction (WAXD), differential scanning calorimetry (DSC), and scanning electron microscopy (SEM). The anisotropic crystalline structure with full concentric circular rings originally shown on the WAXD patterns of the as-prepared and drawn UHMWPE fibers gradually transform into oriented fibers with azimuthal spots on the equator as their DR values increase from 1 to 20, in which their orthorhombic crystals, percentage crystallinity, crystalline orientation, and the birefringence values increase significantly. As evidenced by SEM and WAXD analysis, the chain-folded molecules originally present in kebab crystals of the as-prepared UHMWPE fiber specimens gradually transformed into shish-like crystals with relatively high orientation as their DR values increase from 1 to 20. In contrast, the crystallinity and crystal orientation values of the drawn UHMWPE specimens increase only slightly, as their DR

values increase from 20 to 40, wherein both crystallinity values of orthorhombic and monoclinic crystals increase slightly. In fact, barely any oriented kebab but only shish crystals were observed on the surfaces of drawn UHMWPE fiber specimens with DR values higher than 20. The birefringence values increase only slightly with further increasing DR values, while crystallinity and crystal orientation values of the drawn UHMWPE fiber specimens remained relatively unchanged as their DR values increase from 40 to 150. In the meantime, the monoclinic crystals gradually grow at the expense of the orthorhombic form crystals as the DR values of drawn UHMWPE fiber specimens increase from 40 to 150. Possible reasons accounting for these interesting properties found for the drawn UHMWPE fibers with varying draw ratios are proposed in this study.

Introduction

The gel-spun ultrahigh molecular weight polyethylene (UHMWPE) fiber has attracted great attention based on its low density, solubility properties, and superior mechanical properties with high Young's modulus and tensile strength, especially in the form of drawn films and fibers for many potential industrial applications [1–5]. In general, crystal phase transitions in UHMWPE fibers have been characterized by using wide- and small-angle X-ray diffraction (WAXD and SAXS) [4, 6–15], nuclear magnetic resonance (NMR) [16–19], Fourier transform infrared spectroscopy (FTIR) [20], differential scanning calorimetry (DSC) [13–15, 21], and others [22, 23]. Under ambient condition, the UHMWPE fiber exhibits three phases including crystalline, orientated-intermediate, and amorphous phase [7].

J.-T. Yeh (✉) · S.-C. Lin
Graduate School of Polymer Engineering, National Taiwan
University of Science and Technology, Taipei, Taiwan
e-mail: jyeh@tx.ntust.edu.tw

J.-T. Yeh
Faculty of Chemistry and Material Science, Hubei University,
Wuhan, China

C.-W. Tu · F.-C. Chang
Institute of Applied Chemistry, National Chiao-Tung University,
Hsinchu, Taiwan

K.-H. Hsie
Institute of Polymer Science and Engineering, National Taiwan
University, Taipei, Taiwan

Orthorhombic crystal phases accompanied with small fractions of monoclinic crystalline phases are often found in the crystalline phases of UHMWPE fiber specimens [4, 7, 9]. The molecular chains present in amorphous and oriented-intermediate phases of UHMWPE fibers exhibit a preferred direction parallel to the fiber axis but show no lateral periodicity. The superior mechanical properties of UHMWPE fibers are mainly attributed to their highly oriented orthorhombic phases and intermediary oriented chains [4]. The highest tenacity of commercial available UHMWPE fibers reaches 45 g/den, which is about 10 times higher than those of steel fibers [24].

Multiple melting endotherms were observed on the DSC thermograms of the UHMWPE drawn fiber specimens [14, 25–27]. The main endotherm peak at about 137 °C is originated from the melting of the orthorhombic crystals [28]. Surprisingly, some of the peak melting temperatures are significantly higher than the equilibrium melting temperature (ca. 142 °C) reported for polyethylene crystals. As suggested by Ratner and coauthors [13, 29], the abnormally high melting temperature is due to the melting of constrained orthorhombic crystals present in the UHMWPE specimens. In contrast, a newly developed endotherm observed at peak temperature around 153 °C on the right shoulder of the main melting endotherm is attributed to the transition of the constrained orthorhombic crystals into the hexagonal or pseudohexagonal crystal phases. The obtained hexagonal crystals are then melted at even higher temperatures, and hence, result in another melting endotherm with a peak temperature at around 159 °C [21, 28].

Most of the investigations [14, 25–29] regarding the multiple melting and crystal phase transition properties of the UHMWPE specimens are based on the studies of the commercially available UHMWPE fibers or films. However, the dependence of draw ratios on the morphology and tensile properties of the UHMWPE fibers, the influence of draw ratios of UHPWPE fibers on their thermal and crystal phase transition properties have rarely been reported. In this study, varying draw ratios of UHMWPE fiber specimens were prepared using one- and two-stage drawn processes. The multiple melting, crystal phase transition, orientation, and morphology of the as-prepared and drawn UHMWPE fiber specimens with varying draw ratios were studied. Possible reasons accounting for the improved tensile properties of the ultradrawn UHMWPE fiber specimens are proposed.

Experimental

Materials and sample preparation

The ultrahigh molecular weight polyethylene (UHMWPE) ($M_w = 4.5 \times 10^6$) and low molecular weight polyethylene

(LMWPE) ($M_w = 9.0 \times 10^4$) resins used in this study were kindly supplied by Bruce Lu of Yung Chia Chemical Industrial Corporation (Kaohsiung, Taiwan). As reported in our previous investigations [24–27], the achievable draw ratios of fiber specimens prepared from UHMWPE/LMWPE blends are significantly higher than those of UHMWPE fiber specimens. Presumably, the enormous entanglements present in the UHMWPE gel-network-structures can be significantly reduced after addition of the LMWPE molecules and, hence improve the drawability of the fiber specimens. UHMWPE was mixed with LMWPE at a weight ratio of 98:2, and then dissolved in decalin at 150 °C for 4 h, wherein 0.1 wt% di-*t*-butyl-*p*-cresol was added as an antioxidant. The gel solution thus prepared was then fed into a temperature-controlled hopper and maintained as a hot homogenized solution before spinning. The prepared solution was then gel-spun using a conical die with an exit diameter of 1 mm at an extrusion rate of 3000 mm/min and an extrusion temperature of 150 °C, respectively. A water bath and a winder with 70 mm in diameter were placed at a distance of 200 mm and 650 mm from the spinneret exit, respectively. The extruded gel fibers were cooled in a temperature-conditioned atmosphere and then quenched in a water bath for about 1 min, where temperatures of the air atmosphere and water bath were controlled at 15 °C. The quenched fibers were then extracted in a *n*-hexane bath for 5 min to remove the residual decalin solvent. The extracted fiber specimens were then dried in air for 30 min to remove the remaining hexane solvent before any drawing run.

As reported in the literatures [24–27, 30–35], the temperatures, drawing rates used during the drawing processes can markedly affect the thermal, tensile, drawing properties, and crystalline microstructures of the UHMWPE fiber and film specimens. As reported in our previous investigations [24–27, 30–33], at a fixed drawing rate, the achievable draw ratios of each UHMWPE fiber and/or film specimen was found to reach a maximum value when each specimen was drawn at a temperature near its optimum temperature. The achievable draw ratio of each fiber and/or film specimen drawn at a constant rate and a temperature near T_{op} was referred to as the Dr_{aop} , which reached another maximum value as the drawing rates approached an optimum value. The detailed drawing procedure was described elsewhere in our previous studies [24–27]. In fact, the optimum drawing temperature and rate obtained for each UHMWPE specimen are 95 °C and 20 mm/min, respectively. The Dr_{ra} values of the UHMWPE specimens can be further improved by using a two-stage drawing process, wherein the temperature used in the second drawing stage is higher than 95 °C. After drawing the UHMWPE fiber specimen at the optimum temperature and rate up to a draw ratio of 20, the optimum second stage drawing temperature and rate are

115 °C and 30 mm/min, respectively. By using the optimum two-stage drawing condition, the D_{ra} values of each UHMWPE specimens can be further improved to another maximum value. To prepare the fiber specimens with relatively high draw ratios and different microstructures, the optimum drawing condition used in the one-stage and two-stage drawing process of our previous investigations [24–27] was used to prepare the UHMWPE fiber specimens in this study. The fiber specimens used in the one- and two-stage drawing experiments were cut from the dried as-prepared fibers and then stretched on a Tensilon testing machine (model RTA-1T) equipped with a temperature-controlled oven at a crosshead speed of 20 mm/min. The fiber specimens (30-mm length) were first drawn at 95 °C to a draw ratio of 3, 5, 10, and 20, respectively. The one-stage drawn fiber specimens with a DR value of 20 were then further drawn at 115 °C to the final desired ratio. Tensile properties of the as-prepared and drawn fiber specimens were determined using the Tensilon testing machine at 25 °C and a crosshead speed of 20 mm/min.

Wide-angle X-ray diffraction

The wide-angle X-ray diffraction (WAXD) data for structural analyses of as-prepared and drawn fibers were performed using the wiggler beamline BL17A1 of the National Synchrotron Radiation Research Center (NSRRC) of Taiwan using a triangular bent Si (111) single crystal to obtain a monochromated beam of wavelength $\lambda = 1.3329$ Å. The X-ray diffraction patterns of the as-prepared and drawn fibers were recorded using imaging plate (IP; Fuji BAS III, 20×40 cm²) curved with a radius equivalent to the sample-to-detector distance (280 mm). With 100 μ m pixel resolution of IP and a typical exposure time of 1 min, the WAXD data were measured covering a range of two theta from 15 to 23°. The two theta angle was calibrated according to the diffraction position of standard Si powder. The crystallinities of the as-prepared and drawn UHMWPE fibers were determined from the WAXD patterns. The peak areas of the amorphous phase, orthorhombic and monoclinic crystals for each sample were first fitted from Gaussian function by using the PeakFit simulation software. The crystallinity was then calculated by summing all the peak area fractions of orthorhombic and monoclinic crystals.

Birefringence analysis and crystal orientation

The birefringence properties of the as-prepared and drawn fiber specimens were measured using a polarizing microspectrometer (model TFM-120 AFT). In addition, a quantitative estimate of the degree of orientation in the crystalline phases of UHMWPE fibers can be obtained

through calculation of the Hermans orientation function (f_c , Eq. 1) [36, 37].

$$f_c = \frac{(3\langle \cos^2 \phi \rangle - 1)}{2} \quad (1)$$

The f_c takes the value 1 and $-1/2$ with complete orientation parallel and perpendicular to the drawing direction, respectively. The value of $\langle \cos^2 \phi \rangle$ in Eq. 1 can be calculated from Eq. 2,

$$\langle \cos^2 \phi \rangle = \frac{\int_0^{\pi/2} I_{hkl}(\phi) \sin \phi \cos^2 \phi d\phi}{\int_0^{\pi/2} I_{hkl}(\phi) \sin \phi d\phi} \quad (2)$$

where ϕ is the azimuthal angle and I_{hkl} is the intensity of a specific (hkl) plane, respectively. The (hkl) plane we used here is the orthorhombic peak (110).

Thermal analysis

Thermal properties of as-prepared and drawn fiber specimens were performed on a TA differential scanning calorimeter (DSC) model 2010. All scans were carried out at a heating rate of 3 °C/min over a temperature range from 100 to 200 °C under flowing nitrogen at a flow rate of 25 mL/min. Samples weighing about 0.5 mg were placed in the standard aluminum sample pans for determination of their thermal properties.

Etching treatment

The fiber specimen was agitated ultrasonically at 60 °C with excess amounts of fuming nitric acid. The amorphous regions of the as-prepared and drawn fiber specimens can be etched out to emphasize the crystalline morphology. After the acid treatment for 6 h, the sample was washed by de-ionized water, boiling acetone, and then dried at room temperature. The surface morphology of the treated specimen was characterized by scanning electron microscopy (SEM) (JOEL JSM 6500F Tokyo, Japan) at 5 kV.

Results and discussion

X-ray diffraction properties

Figure 1 presents the WAXD of the as-prepared, one- and two-stage drawn UHMWPE fibers with DR values varying from 1 to 150. In addition to the broad amorphous hump ranging from $2\theta = 15$ – 20° , two distinct diffraction peaks corresponding to (110)_o and (200)_o planes of the orthorhombic crystals at $2\theta = 18.2^\circ$ and 20.4° , respectively, were found on the WAXD patterns of the as-prepared and

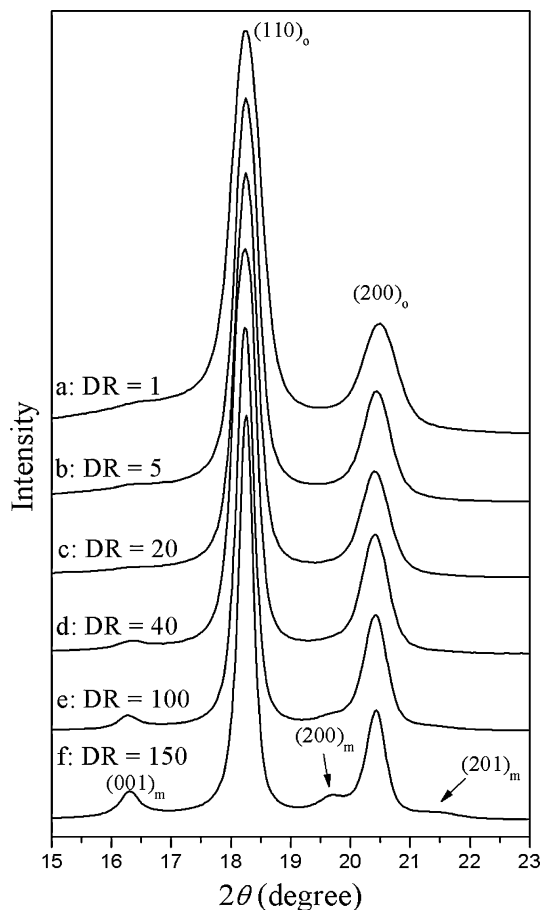


Fig. 1 WAXD patterns of as-prepared and drawn UHMWPE fiber specimens with DR values of (a) 1, (b) 5, (c) 20, (d) 40, (e) 100, and (f) 150

drawn UHMWPE fiber specimens. It is worth noting that a minor diffraction peak at $2\theta @ 16.3^\circ$ corresponding to the monoclinic $(001)_m$ diffraction was found on the WAXD patterns of the drawn UHMWPE fiber specimens in which the monoclinic $(001)_m$ diffraction peaks become more pronounced as their DR values increase from 1 to 150. Another monoclinic $(200)_m$ and $(201)_m$ diffraction peaks at $2\theta = 19.7$ and 21.5° [15] were also observed as the DR values of the two-stage drawn UHMWPE fibers are higher

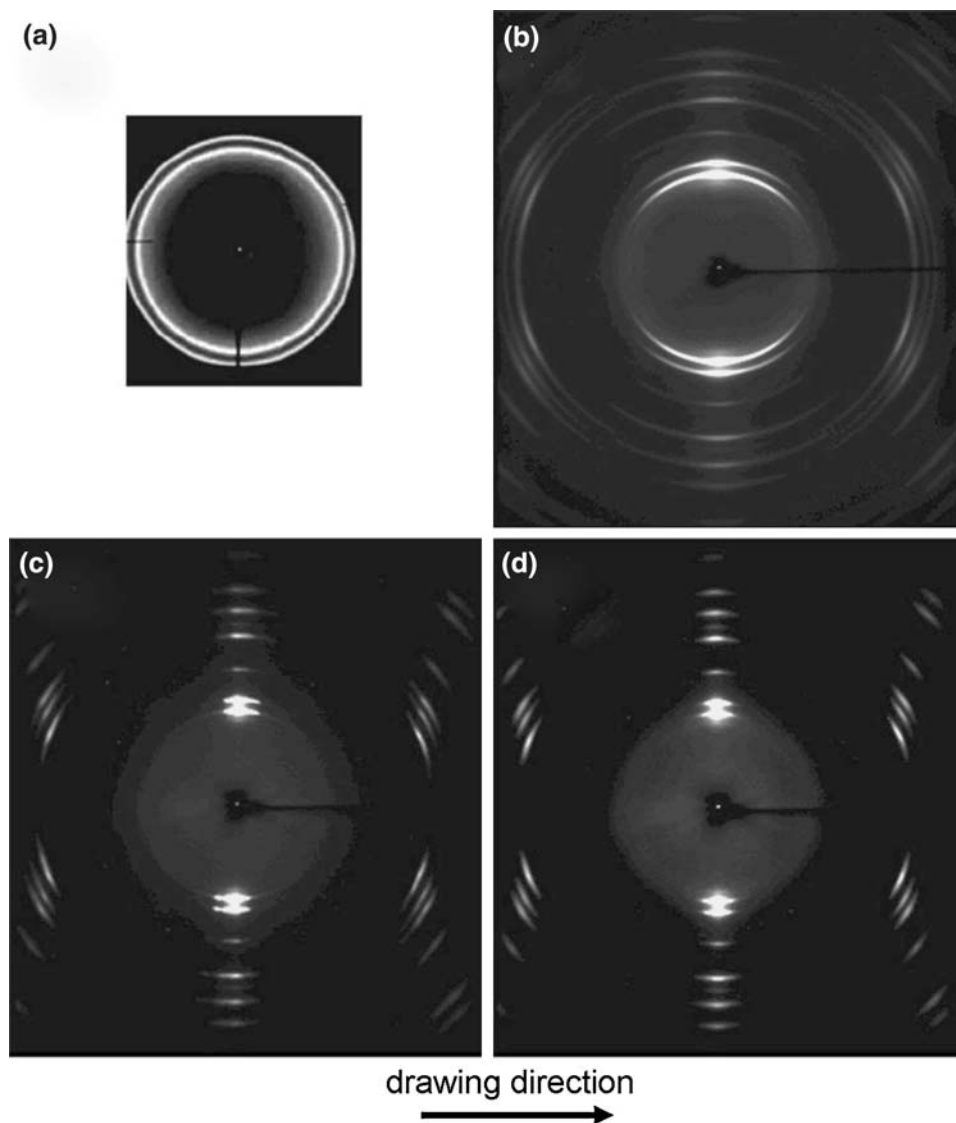
than 100. As shown in Table 1, the crystallinity values (Vc) estimated corresponding to the summations of the orthorhombic and monoclinic diffraction areas increase with the increasing DR. The Vc values of UHMWPE fiber specimens increase rapidly from 78.7% to 94.5% as their DR values increase from 1 to 20, wherein most of the increase in Vc values is due to the formation of orthorhombic crystals, the Vc values corresponding to the monoclinic crystals remain nearly unchanged as their DR values increase from 1 to 20 (see Table 1). In contrast, the Vc values of UHMWPE fiber specimens increase by only 2.8%, as their DR values increase from 20 to 150. In which, the Vc values corresponding to the monoclinic and orthorhombic crystals increase and reduce gradually from 0.6% to 10.9% and 93.9% to 86.4%, respectively, as their DR values increase from 20 to 150.

Figure 2 shows selected two-dimensional X-ray (2D X-ray) diffraction patterns of the as-prepared and drawn UHMWPE fiber specimens. Full concentric circular rings were found on the 2D X-ray patterns of the as-prepared UHMWPE fiber specimens, indicating that the crystals present in the as-prepared UHMWPE fiber specimens are isotropic and randomly oriented phases. The full concentric circular rings gradually transform into distinct azimuthal arcs as the DR values increase from 1 to 5 (see Fig. 2b), wherein the diffraction intensity along each azimuthal arc reaches the maximal on the equator. The azimuthal arcs then gradually transform into discrete spots as the DR values of the drawn UHMWPE fiber specimens reach about 20 (see Fig. 2c). At DR values higher than 20, the 2D X-ray diffraction patterns of the drawn UHMWPE fiber specimens remain relatively unchanged (see Figs. 2c and 2d). These results suggest that the isotropic and randomly oriented crystals originally present in the as-prepared fiber specimen gradually orient along the drawing direction as their DR values increase from 1 to 20. In the meantime, the “stress-induced” and newly formed orthorhombic crystals during the drawing processes of UHMWPE fibers are highly oriented along the drawing direction that may also result in discrete azimuthal arcs or spots shown on the 2D X-ray diffraction patterns of the drawn UHMWPE fiber

Table 1 Crystallinities, orthorhombic crystals, and monoclinic crystals (%) of drawn UHMWPE fibers calculated from XRD data

Draw ratio	Amorphous (%)	Orthorhombic crystals (%)		Monoclinic crystals (%)			Crystallinity (%)
		(110)	(200)	(001)	(200)	(201)	
1D	21.3	60.4	17.3	1.0	–	–	78.7
5D	16.6	63.9	18.7	0.8	–	–	83.4
20D	5.5	68.5	25.4	0.6	–	–	94.5
40D	4.4	67.6	26.5	1.5	–	–	95.6
100D	3.0	66.6	27.3	2.1	1.0	–	97.0
150D	2.7	63.7	22.7	5.5	4.6	0.8	97.3

Fig. 2 2D X-ray diffraction patterns of as-prepared and drawn UHMWPE fiber specimens with DR values of (a) 1, (b) 5, (c) 20, and (d) 100 (the fiber axis is in horizontal direction)



specimens. However, at DR values higher than 20, most of these UHMWPE crystals present in the drawn UHMWPE fibers were highly aligned along the drawing direction; further drawing did not improve the crystal orientation noticeably on the 2D X-ray patterns.

Birefringence, crystal orientation, and tensile properties

Figure 3 plots the crystalline orientation (f_c) and the birefringence (f_t) values of as-prepared and drawn UHMWPE fiber specimens versus their DR values. The f_t values of the drawn UHMWPE fibers initially increase rapidly from 0.005 to 0.04 as the DR values increase from 1 to 20. The increasing rates of f_t values reduce significantly, when the DR values of the drawn fibers increase from 20 to 60. At DR values higher than 60, the increasing trends of f_t values slow down to a relatively low but constant value. Similar improvement of the f_c values was found through

calculation of the Hermans orientation function of the $(110)_o$ plane of the orthorhombic crystals present in drawn UHMWPE fiber specimens. The f_c values increase rapidly from 0 to 0.95, as the DR values of the UHMWPE fiber specimens increase from 1 to 20. In contrast, the f_c values of drawn UHMWPE fiber specimens remain relatively unchanged at about 0.96 as their DR values are higher than 20. Apparently, both degrees of orientation of UHMWPE molecules present in amorphous and crystalline phases of drawn fibers improve rapidly as their DR values increase from 1 to 20. However, nearly no improvement in the degrees of orientation of UHMWPE molecules present in the crystalline phases of the drawn fiber specimens can be found as their DR values are higher than 20.

Figure 4 plots tensile moduli and strengths of as-prepared and drawn UHMWPE fiber specimens versus their DR values. Both tensile moduli and strengths of as-prepared and drawn UHMWPE fiber specimens were found to

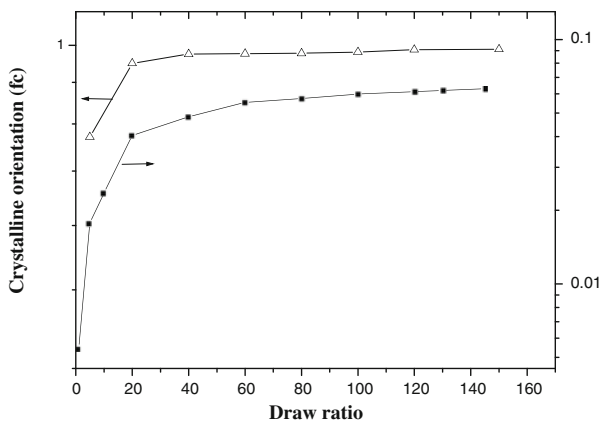


Fig. 3 The crystal orientation (Δ) and birefringence (\blacksquare) values of as-prepared and drawn UHMWPE fiber specimens with varying DR values

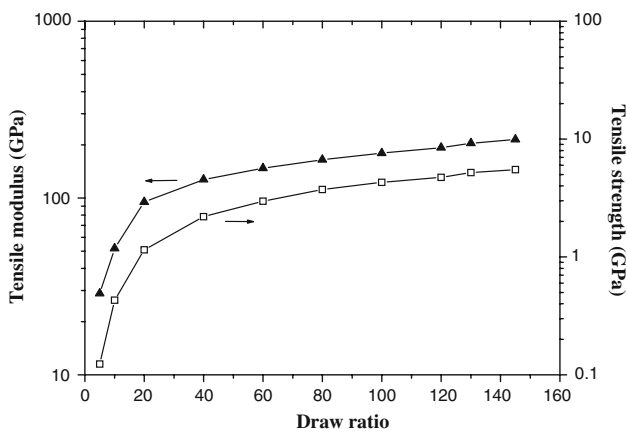


Fig. 4 The tensile moduli (\square) and tensile strengths (\blacktriangle) of as-prepared and drawn UHMWPE fiber specimens with varying DR values

improve consistently as DR values increase from 1 to 20. The increasing trends of tensile moduli and strengths slow down slightly at DR values between 20 and 40 and then remain at a relatively low and constant value as the DR values are higher than 40.

SEM analysis

Figures 5 and 6, 7 presents typical low- and high-magnification SEM micrographs of the etched drawn UHMWPE fiber specimens, respectively. As shown in Fig. 6a–6d, the etched section areas shown on the surfaces of the drawn UHMWPE fiber specimens reduce significantly as the DR values increase from 3 to 20, wherein the etched sections represent the amorphous phases of UHMWPE being etched out after nitric acid treatment. At DR values equal to or higher than 20, one can hardly see the etched spots on the drawn UHMWPE fiber specimens. In contrast, the crystal

phases remain nearly intact on the surfaces of the drawn UHMWPE fiber specimens, wherein the shish and kebab crystals lie roughly parallel and perpendicular to the drawing direction of the drawn UHMWPE fiber specimen, respectively (see Fig. 6a and 6b). As shown in Fig. 6a, 20–50 nm thickness and 360–400 nm width values of the kebab chain-folded lamellar crystals were found on the surfaces of the drawn UHMWPE fiber specimens with a DR value of 3, respectively. However, the kebab crystals present in UHMWPE fiber specimens with relatively low DR values were not well oriented in a direction perpendicular to the fiber drawing direction (see Fig. 6a). The orientations of kebab crystals gradually transform into a direction perpendicular to the fiber drawing direction as their DR values increase from 3 to 20 (see Fig. 6a–6c). However, at DR values higher than 20, the original kebab crystals were transformed and merged into the shish core crystals of the drawn UHMWPE fiber specimens, wherein the kebab crystals could be barely found (see Fig. 6c and 6d).

The morphological, birefringence, and WAXD results found above indicate that the amorphous phases present in UHMWPE fiber specimens reduce and transform quickly into the oriented orthorhombic crystalline phases as the DR values increase up to 20. On the other hand, as evidenced by morphological and WAXD analysis, the improved crystalline orientations of UHMWPE fiber specimens is due to the gradually transformed orientation of the kebab crystals as their DR values increase from 1 to 20.

Thermal properties

The main melting endotherm with a peak temperature at about 132 °C was found for the as-prepared UHMWPE fiber specimen. It is worth noting that the peak temperature associated with the main melting endotherm increases significantly with the increase in draw ratio, which is generally assigned as the melting temperature of the orthorhombic crystals [13, 21, 29, 38]. On the other hand, at DR values near 20, two small but newly developed melting endotherms at temperatures around 148 and 154 °C were found on the right hand side of the main melting endotherms of the drawn UHMWPE fiber specimens. The magnitudes and peak melting temperatures of the two newly developed endotherms increase with further increase in the DR values. However, in contrast to the endotherms with lower melting temperatures, the peak melting temperatures of the newly developed endotherms with higher melting temperatures remain constantly as the DR values of the drawn UHMWPE fiber specimens increase from 20 to 150. For instance, the lower and higher melting temperatures of the two newly developed endotherms increase by about 4 and 0.5 °C, respectively, as the DR values of the drawn UHMWPE fiber

Fig. 5 Low-magnification SEM micrographs of the UHMWPE fibers with DR values of (a) 3, (b) 5, (c) 20, and (d) 40

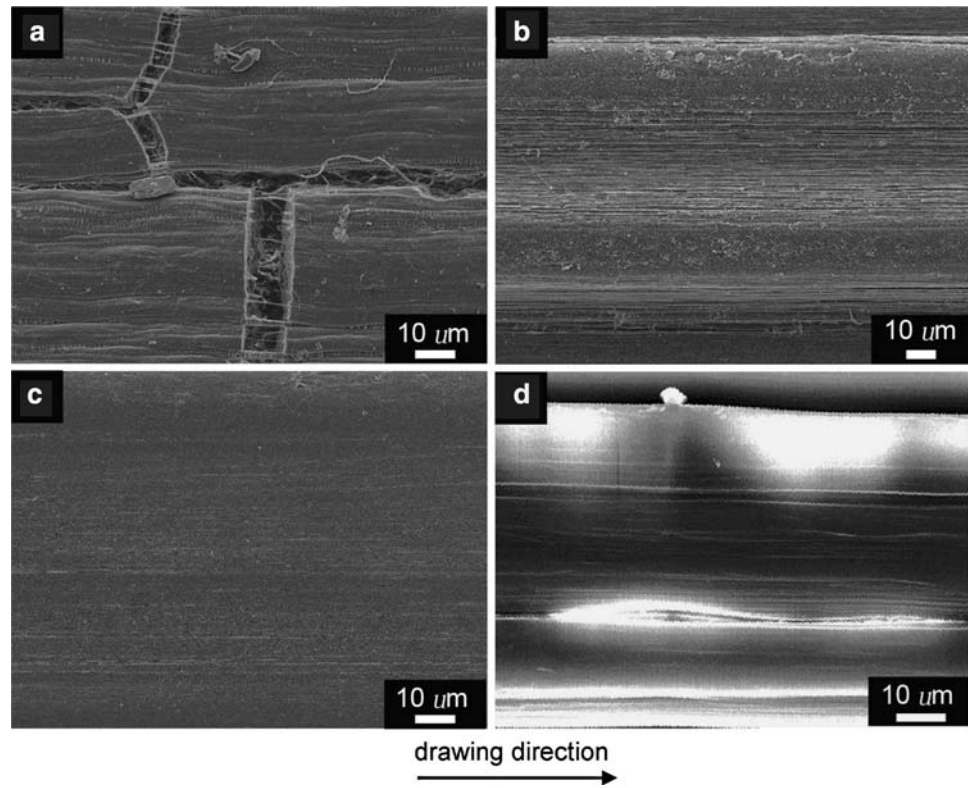
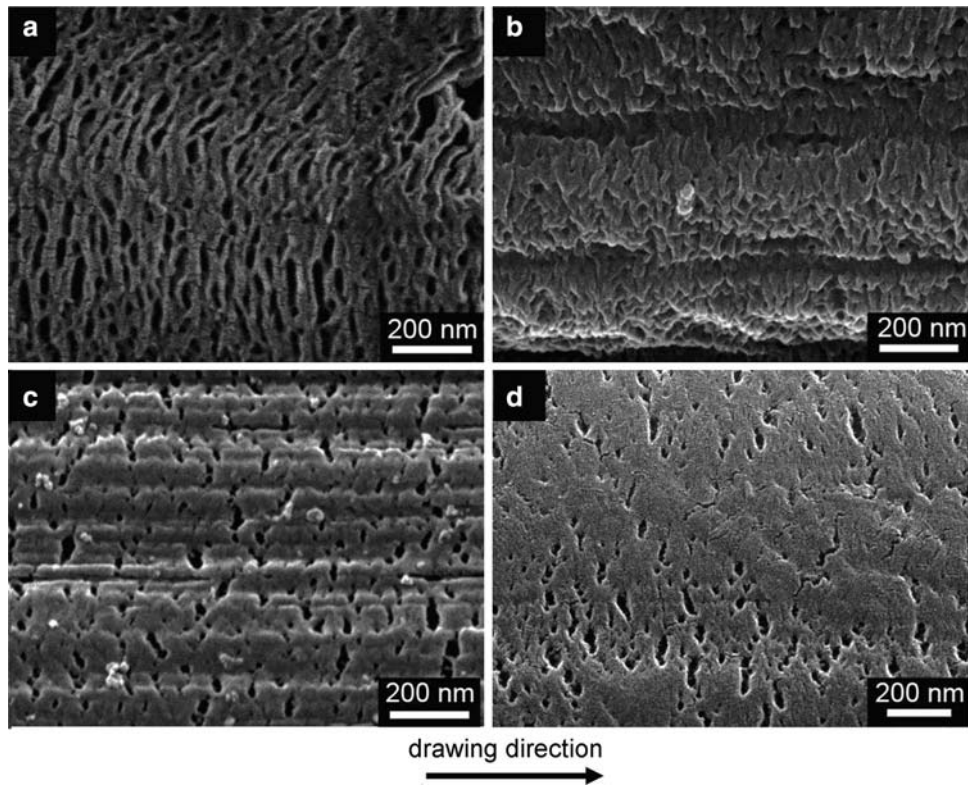


Fig. 6 High-magnification SEM micrographs of the UHMWPE fibers with DR values of (a) 3, (b) 5, (c) 20, and (d) 40



specimens increase from 20 to 150. As reported by several investigations [13, 21, 29, 38], the newly developed melting endotherms with melting temperatures at around 148 °C are

associated with the transition of the constrained orthorhombic crystals into the hexagonal or pseudo-hexagonal crystal phases during the heat-scanning processes. The

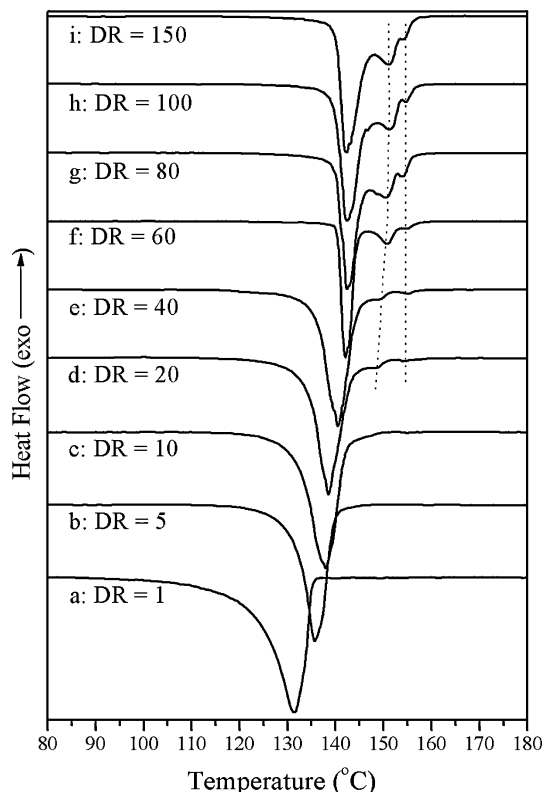


Fig. 7 DSC thermograms of UHMWPE fiber specimens with draw ratios of (a) 1, (b) 5, (c) 10, (d) 20, (e) 40, (f) 60, (g) 80, (h) 100, and (i) 150

higher endotherms with peak melting temperatures at about 154 °C are then attributed to the melting of hexagonal crystals, which are less dependent of DR values of drawn UHMWPE fiber specimens.

In contrast, melting of monoclinic crystals was not detected in the DSC analyses, although their presence in the as-prepared and drawn UHMWPE fiber specimens was confirmed by the WAXD analysis reported in the previous section. However, the melting temperatures of the monoclinic crystals are roughly in the ranges of those of the orthorhombic crystals, and less than 3.1% of monoclinic crystals were found on the drawn UHMWPE fibers even when their draw ratios approach 100. Based on these premises, the lack of distinguished melting endotherms of monoclinic crystals is likely due to the overlapping the relatively small melting endotherm of the monoclinic crystals on the orthorhombic melting endotherms of the as-prepared and drawn UHMWPE fiber specimens. Similar results were found by Ratner et al. [13].

These interesting WAXD, birefringence, crystal orientation, morphology, and thermal properties of the as-prepared and drawn UHMWPE fibers suggest that many of the UHMWPE molecules originally present in the amorphous phases of as-prepared UHMWPE fiber

specimens were likely activated by stress crystallization and transformed into oriented orthorhombic crystals or highly oriented molecules as the DR values increase from 1 to 20. As a consequence, the crystallinity and birefringence values of the drawn fiber specimens increase significantly from 78.7% to 94.5% and 0.005 to 0.04, respectively, as their DR values increase from 1 to 20. As evidenced by SEM and WAXD analysis, the chain-folded molecules originally present in kebab crystals of the as-prepared UHMWPE fiber specimens gradually transformed into shish-like crystals with relatively high orientation as their DR values increase from 1 to 20 and hence result in a significant increase in crystal orientation values during this drawing period. In contrast, the crystallinity and crystal orientation values of the drawn UHMWPE specimens increase still significantly from 94.5% to 95.6% and 0.95 to 0.96, respectively, as their DR values increase from 20 to 40, wherein both crystallinity values of orthorhombic and monoclinic crystals increase slightly with the increase in DR values. The small (c.a. 1%) increase in crystallinity resulted from a significant reduction of the amorphous portion by about 20%. In fact, barely any oriented kebab but only shish crystals were observed on the surfaces of drawn UHMWPE fiber specimens with DR values higher than 20. These interesting results suggest that only small portions of UHMWPE molecules remained in the amorphous phases of UHMWPE drawn fiber specimens were stress-induced and crystallized into either highly oriented orthorhombic or monoclinic crystals and hence, result in small but still significant change in crystallinity and crystal orientation values as the DR values of the UHMWPE drawn fiber specimens increase from 20 to 40. Finally, the birefringence values increase only slightly with further increasing DR values, while crystallinity and crystal orientation values of the drawn UHMWPE fiber specimens remained relatively unchanged as their DR values increase from 40 to 150. In the meantime, it is worth noting that the monoclinic crystals gradually grow at the expense of the orthorhombic form crystals as the DR values of drawn UHMWPE fiber specimens increase from 40 to 150. Presumably, very few UHMWPE molecules remained in the amorphous phases of UHMWPE drawn fiber specimens were stress-induced and crystallized into highly oriented orthorhombic or monoclinic crystals as the DR values of drawn UHMWPE fiber specimens increase from 40 to 150. Small but still significant increase in crystallinity and crystal orientation was observed by the transformation process of orthorhombic UHMWPE crystals into monoclinic crystals during this drawing period. However, the tensile properties of the drawn UHMWPE fiber specimens still improve with the slightly improved birefringence properties of the drawn fiber specimens as their DR values increase from 40 to 150.

Conclusions

The anisotropic crystalline structure with full concentric circular rings originally shown on the WAXD patterns of the as-prepared UHMWPE fibers gradually transform into oriented fibers with azimuthal spots on the equator as the DR values increase from 1 to 20, in which their percentage crystallinity, crystalline orientation, and the birefringence values increase significantly from 78.7% to 94.5%, 0 to 0.95, and 0.005 to 0.04, respectively. As evidenced by SEM and WAXD analysis, the chain-folded molecules originally present in kebab crystals of the as-prepared UHMWPE fiber specimens gradually transformed into shish-like crystals with relatively high orientation as their DR values increase from 1 to 20. In contrast, the orthorhombic and monoclinic crystallinity and crystal orientation values of the drawn UHMWPE fiber specimens increase still significantly, as their DR values increase from 20 to 40. The abnormally high melting temperatures (148–154 °C) found on the newly developed endotherms of the drawn UHMWPE fiber specimens with DR values greater than 20 are attributed to the transition of the constrained orthorhombic into hexagonal crystals and the melting of the hexagonal crystals. The birefringence values increase only slightly with further increasing DR values of the drawn UHMWPE fiber specimens from 40 to 150, while crystallinity and crystal orientation values remained relatively unchanged. In the meantime, the monoclinic crystals gradually grow at the expense of the orthorhombic form crystals as the DR values of drawn UHMWPE fiber specimens increase from 40 to 150. However, the tensile properties of the drawn UHMWPE fiber specimens still improve significantly with the slightly improved birefringence properties of the drawn fiber specimens as their DR values increase from 40 to 150.

Acknowledgements The authors would like to express their appreciation to National Science Council (NSC 95–2221-E-253-008-MY3) and Department of Industrial Technology, Ministry of Economic Affairs (95-EC-17-A-11-S1-057) for their support of this work. Thanks are also extended to Drs. M. H. J. Koch, A. Gabriel, Y. S. Sun, and Y. H. Lai for their help in WAXS measurements.

References

- Smith P, Lemstra PJ (1979) *Macromol Chem* 180:2983. doi:10.1002/macp.1979.021801220
- Barham PJ, Leller A (1985) *J Mater Sci* 20:2281. doi:10.1007/BF00556059
- Ward IM (1995) *Macromol Symp* 100:1
- Poter RS (1980) *Chem Rev* 80:351. doi:10.1021/cr60326a005
- Rudin A, Tchir WJ, Gagnon R, Schreiber HP, Collacoot R (1989) *Ind Eng Chem Res* 28:174. doi:10.1021/ie00086a008
- Mooen JA, Kip BJ (1992) *J Polym Sci Part B: Polym Phys* 30:361. doi:10.1002/polb.1992.090300406
- Riekel C, Cedola A, Heidelbach F, Wagner K (1997) *Macromolecules* 30:1033. doi:10.1021/ma960799s
- Yang L, Somani RH, Sics I, Hsiao BS, Kolb R, Fruitwala H, Ong C (2004) *Macromolecules* 37:4845. doi:10.1021/ma049925f
- Russel KE, Heyding RD (1997) *Polymer* 38:1409. doi:10.1016/S0032-3861(96)00643-X
- Nakae M, Uehara H, Kanamoto T, Zachariades AE, Porter RS (2000) *Macromolecules* 33:2632. doi:10.1021/ma991330a
- Hu XP, Hsieh YL (1998) *Polym J* 30:771. doi:10.1295/polymj.30.771
- Hsieh YL, Ju J (1994) *J Appl Polym Sci* 53:347. doi:10.1002/app.1994.070530312
- Ratner S, Weinberg A, Maron G (2003) *Polym Compos* 24:422. doi:10.1002/pc.10040
- Ratner S, Weinberg A, Wachtel E, Moret PM, Maron G (2004) *Macromol Rapid Commun* 25:1150. doi:10.1002/marc.200400102
- Luo C, Guardala NA, Price JL, Chodak I, Zimmerman O, Weiss RG (2002) *Macromolecules* 35:4690. doi:10.1021/ma020235q
- Hu WG, Schmidt RK (2000) *Polymer* 41:2979. doi:10.1016/S0032-3861(99)00429-2
- Rotzinger BP, Chanzy HD, Smith P (1989) *Polymer* 30:1814. doi:10.1016/0032-3861(89)90350-9
- Vanderhart DL, Khoury F (1984) *Polymer* 25:1589. doi:10.1016/0032-3861(84)90151-4
- Uehara HM, Aoike HT, Yamanobe T, Komoto T (2001) *Polymer* 42:5893. doi:10.1016/S0032-3861(00)00911-3
- Sheiko S, Frey H, Moller M (1992) *Colloid Polym Sci* 270:440. doi:10.1007/BF00665987
- Kwon YK, Boller A, Pyda M, Wunderlich B (2000) *Polymer* 41:6237. doi:10.1016/S0032-3861(99)00839-3
- Silverstein MS, Sadovsky J, Alon D, Wahad V (1999) *J Appl Polym Sci* 72:405. doi:10.1002/(SICI)1097-4628(19990418)72:3<405::AID-APP10>3.0.CO;2-I
- Zhang H, Shi M, Zhang J, Wang S (2003) *J Appl Polym Sci* 89:2757. doi:10.1002/app.12448
- Yeh JT, Chang SS (2000) *J Mater Sci* 35:3227. doi:10.1023/A:1004858902462
- Yeh JT, Lin YT, Jiang HB (2003) *J Appl Polym Sci* 91:1559. doi:10.1002/app.13259
- Yeh JT, Chang SS (2001) *J Appl Polym Sci* 79:1890. doi:10.1002/1097-4628(20010307)79:10<1890::AID-APP180>3.0.CO;2-T
- Yeh JT, Lin YT, Chen KN (2003) *J Appl Polym Sci* 89:3728. doi:10.1002/app.12390
- Chodak I (1998) *Prog Polym Sci* 23:1409. doi:10.1016/S0079-6700(98)00006-9
- Alon Y, Maron G (2004) *Macromol Rapid Commun* 25:1387. doi:10.1002/marc.200400185
- Yeh JT, Chang SS, Yen MS (1998) *J Appl Polym Sci* 70:149. doi:10.1002/(SICI)1097-4628(19981003)70:1<149::AID-APP15>3.0.CO;2-2
- Yeh JT, Chang SS (2002) *Polym Eng Sci* 42:1558. doi:10.1002/pen.11051
- Jiang T, Shyu WD, Lin YT, Chen KN, Yeh JT (2003) *Polym Eng Sci* 43:1765. doi:10.1002/pen.10149
- Yeh JT, Lin YT, Chen KN (2003) *J Polym Res* 10:55. doi:10.1023/A:1023961216058
- Kanamoto T, Tsuruta A, Tanana K, Takeda M, Porter RS (1988) *Macromolecules* 21:470. doi:10.1021/ma00180a032
- Smook J, Pennings AJ (1982) *J Appl Polym Sci* 27:2209. doi:10.1002/app.1982.070270631
- Hermans PH (1949) *J Polym Sci* 4:749. doi:10.1002/pol.1949.120040609
- Stein RS (1958) *J Polym Sci* 31:327. doi:10.1002/pol.1958.1203112309
- Lacroix FV, Schulte K (1999) *Polymer* 40:843. doi:10.1016/S0032-3861(98)00309-7